Characterization of defects in multicrystalline silicon solar cell mesa diodes

NM Thantsha, FJ Vorster and EE van Dyk
Department of Physics, PO Box 77000, Nelson Mandela Metropolitan University, Port Elizabeth, 6031, South Africa

Abstract

In this paper a simple, inexpensive and fast procedure for the fabrication of mesa diodes on multicrystalline silicon (mc-Si) solar cell is discussed. Mesa diodes are achieved by etching a solar cell so that predefined plateau regions are formed. These mesa diodes expose the p-n junction and provide a better way of determining and analysing the fundamental current conduction mechanisms at the junction. The purpose of this study is to illustrate the usefulness of the procedure to determine the spatial distribution of device parameters and defects. A method which uses the mesa diodes for the characterization of defects is described and the results show that the effect of grain boundaries (GBs) and how surface reflection defects compromise the photo response of mc-Si solar cells. The parameters of the current-voltage characteristics revealed that the behaviour of the mesa diodes is affected by defects. The simplicity of the procedure facilitates the investigation of any region of interest on a mc-Si solar cell with relative ease and the mesa diodes can be fabricated in a short time.

Keywords: Mesa diodes, solar cell, grain boundary, performance parameters

1. Introduction

The defects inherent to multicrystalline silicon give rise to performance limiting effects in solar cell wafers manufactured from such material (Warta 2002). Although defects such as grain boundaries are distributed throughout the wafers, there are also regions of material with higher concentrations of defects. The recombination processes and also carrier transport near and at a grain boundary have been widely researched. Various theoretical models showed that grain boundary interface states determine the electrical and photovoltaic properties of mc-Si by acting as carrier traps and recombination centres (Gosh et al. 1980, Donolato 1983, Meng et al. 2000). Topographical measurement techniques such as Laser Beam Induced Current (LBIC) have been used to evaluate the electrical characteristics of solar cells and investigate the photogenerated current profile at a grain boundary (Marek 1984, Mattiga et al. 1988). LBIC is a technique for diagnosing electrical defects in solar cells (Donolato 1983). This paper presents a method of investigating the effect of current limiting defects in mc-Si cells by electrically isolating and characterizing defect containing regions. We have developed a technique to produce mesa diodes on a processed wafer in order to electrically isolate specific regions of the solar cell that are of interest. The method of studying spatial non-uniformities by isolating specific areas on crystalline solar cells is not unique and this article demonstrates the value of the mesa processing technique. Sopori (1988), for example, used a process where an array of mesas and junction diffusion are produced in sequence. In our work we typically have a completed solar cell that we wish to characterize with respect to material parameter in regions of interest. In principle, this study presents a procedure which enables the fabrication of mesa diodes so that LBIC investigations can be performed. This technique enables us to study spatial distribution of material and device parameters in solar cells. In order to create mesas of repeatable size and with strain free cell material at the edges, a wax-etch technique with a vinyl

mask to define the mesa areas was used. In this study, mesa diodes on multicrystalline Si (mc-Si) solar cells were prepared and subsequently analyzed using LBIC measurements and current-voltage (I-V) characteristics.

2. Experimental details

The method of melting the wax onto a heated sample to mask the selected mesa diode from etching is a quick and efficient way to define an area of interest for analysis. The disadvantage is that it is difficult to control the wax flow, and hence the waxed area varies from diode to diode. Also, during the etching process, areas under the wax-defined regions are often etched, resulting in an irregular shape around the edges. In addition, the rough surface texture of a mc-Si cell does not allow the use of a metal mask as is commonly used for single crystalline material, since the wax may flow between the metal mask and mc-Si solar cell sample. This problem is solved by using masks made by cutting the required array of holes in a sheet of self-adhesive vinyl. The mask may be cut to the required size and pasted on to the sample with the openings aligned with the areas to be investigated. In this study, black wax was dissolved in toluene and sprayed onto vinyl masked samples using an artist's spray gun. The process of preparing the samples, i.e. spraying, etching and cleaning takes less than half an hour. This process is illustrated in Fig. 1, with the mesas prepared as follows (refer to Fig. 1):

(a) Vinyl mask is pasted on to the front surface of the cell and wax melted on to the back contact to protect the area from etching;
(b) Wax is sprayed on to the surface of the masked cell and allowed to dry;
(c) Mask is removed leaving the waxed areas;
(d) The cell is etched to a depth below the p-n junction in a HNO_3:HF solution with a volume ratio of 5:1;
(e) Wax is removed by boiling in toluene, and then the cell is cleaned in methanol followed by rinsing in de-ionized water and dried with nitrogen.

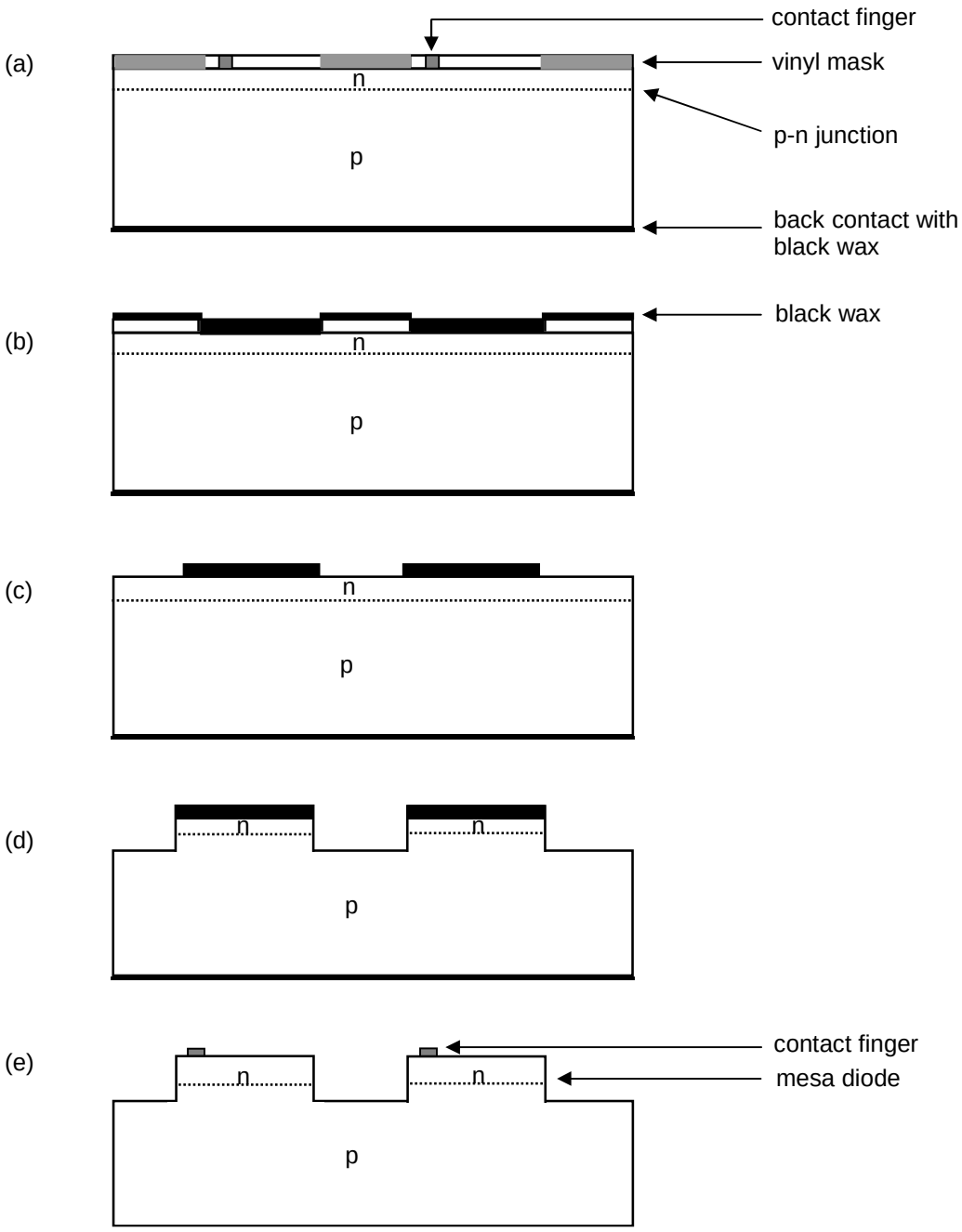

Figure 1: Schematic diagram of the processing steps during mesa preparation.

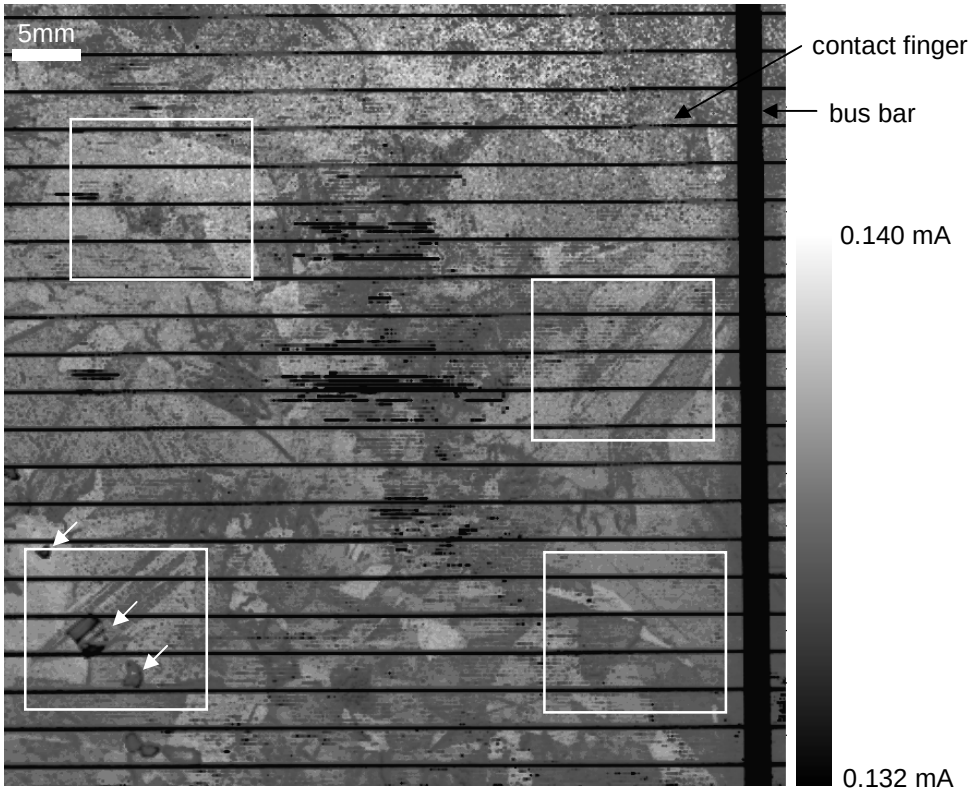

Figure 2: LBIC map of $6 \times 6\ \mathrm{cm}^2$ mc-Si solar cell using beam diameter of 150 μm and step size of 150 μm. The relative photocurrent scale is also shown.

Figure 2 shows an LBIC map of a 6 x 6 cm^2 mc-Si solar cell with bus bar and contact fingers clearly visible. The 1 mm diameter mesa diodes were developed on the mc-Si solar cell shown in Fig. 2. The areas where mesa diodes were created were chosen to coincide with areas of interest as revealed by LBIC maps which indicate variations in the photo response of the mc-Si solar cell. Mesa diodes were intentionally created around, for instance, grain boundaries in order to investigate local defects. An LBIC system with laser light of wavelength 660 nm was used to analyze defects within the mc-Si solar cell mesa diodes. At this wavelength silicon solar cells reflect 20% of the 660 nm wavelength light (Goetzeberger, Knobloch & Voss 1998, pp. 84-85) and the light remaining penetrates to a depth of about 3.5 μm. This makes it possible to detect and analyse defects on the surface and within the penetration depth. The results of the LBIC measurements were obtained using focused laser light with a diameter ranging between 100 μm and 150 μm and scanning step size between 150 μm and 50 μm. The laser light incident on the mesa diode produces an induced current, and by scanning the surface of the mesa an LBIC map of the mesa diode was obtained. In addition, dark and illuminated current-voltage (I-V) characteristics of the mesa diodes were also obtained. The dark I-V measurements were performed by biasing the mesa diode with a dc voltage source under dark conditions. The biasing voltage was in the range, $-3\,V < V_{bias} < 0.5\,V$. The light I-V measurements were obtained using defocused 660 nm laser with a beam intensity of 30 mW/cm^2 to illuminate the whole mesa. The I-V characteristic curves were then measured by biasing the mesa from reverse to forward

bias in the range, $-2\,V < V_{bias} < 0.8\,V$ using an external ac voltage source with a frequency of 22 Hz and measuring the photogenerated current at preset voltages. The open-circuit voltage V_{oc}, short-circuit current I_{sc} were obtained directly from the I-V curves and the device parameters were extracted by employing a Particle Swarm Optimization (PSO) iteration method based on the one-diode model of a solar cell (Macabebe & van Dyk 2008). These parameters include reverse saturation current I_0, ideality factor n, series resistance R_s and shunt resistance R_{sh}.

3. Results and discussion

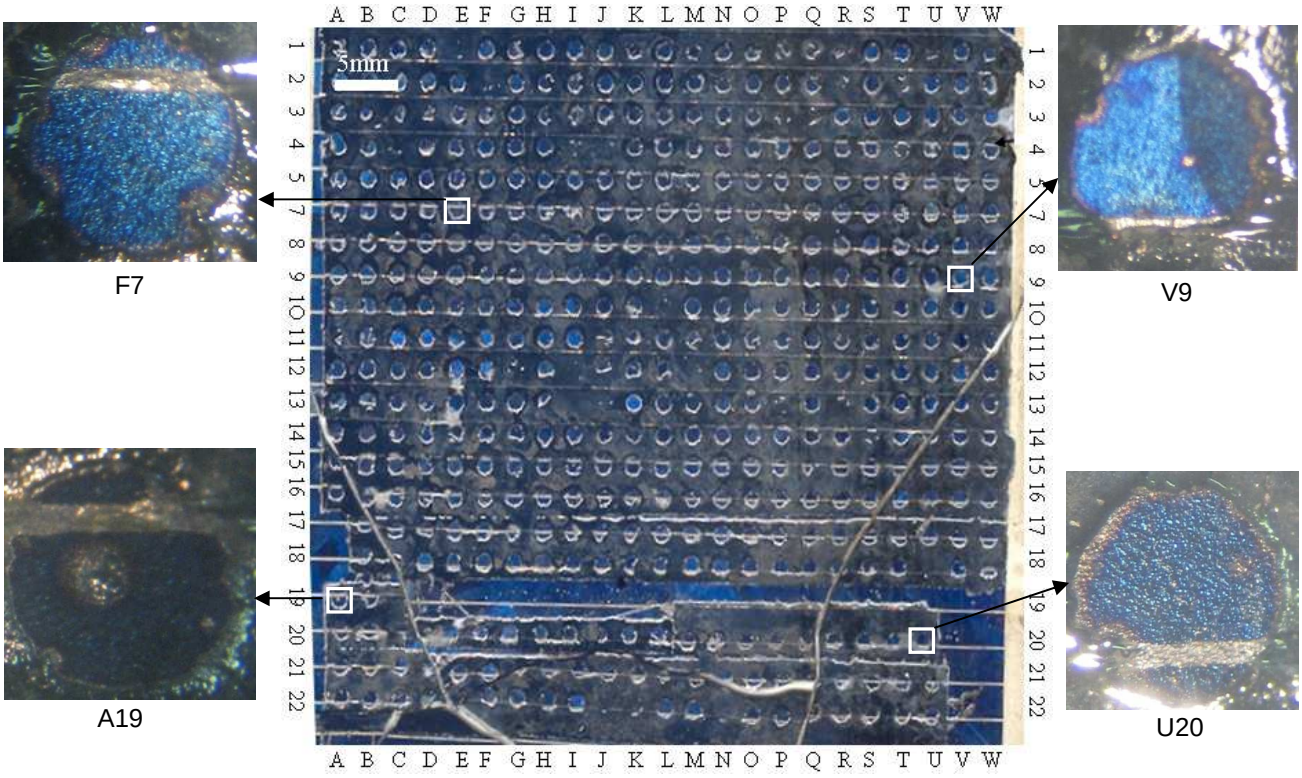

Figure 3: Photograph of the mesa diode developed on mc-Si solar cell in Figure 2.

Fig. 3 shows 1 mm diameter mesa diodes created on the mc-Si solar cell sample shown in Fig. 2. From Fig. 3, contact fingers are evident on some of the mesa diodes. During current collection, the fingers provide front contacts while the back side of the whole mc-Si solar cell sample provides a common rear contact. This study presents and analyzes results of LBIC and I-V measurements on the mc-Si solar cell mesa diodes selected from the areas marked in the squares in Fig. 2. In the selected areas, mesas F7, A19, V9 and U20 were analyzed. The reason for selecting these mesas was to investigate carrier transport within different areas of the whole solar cell. For example, grain boundary areas, finger areas, edges, etc.

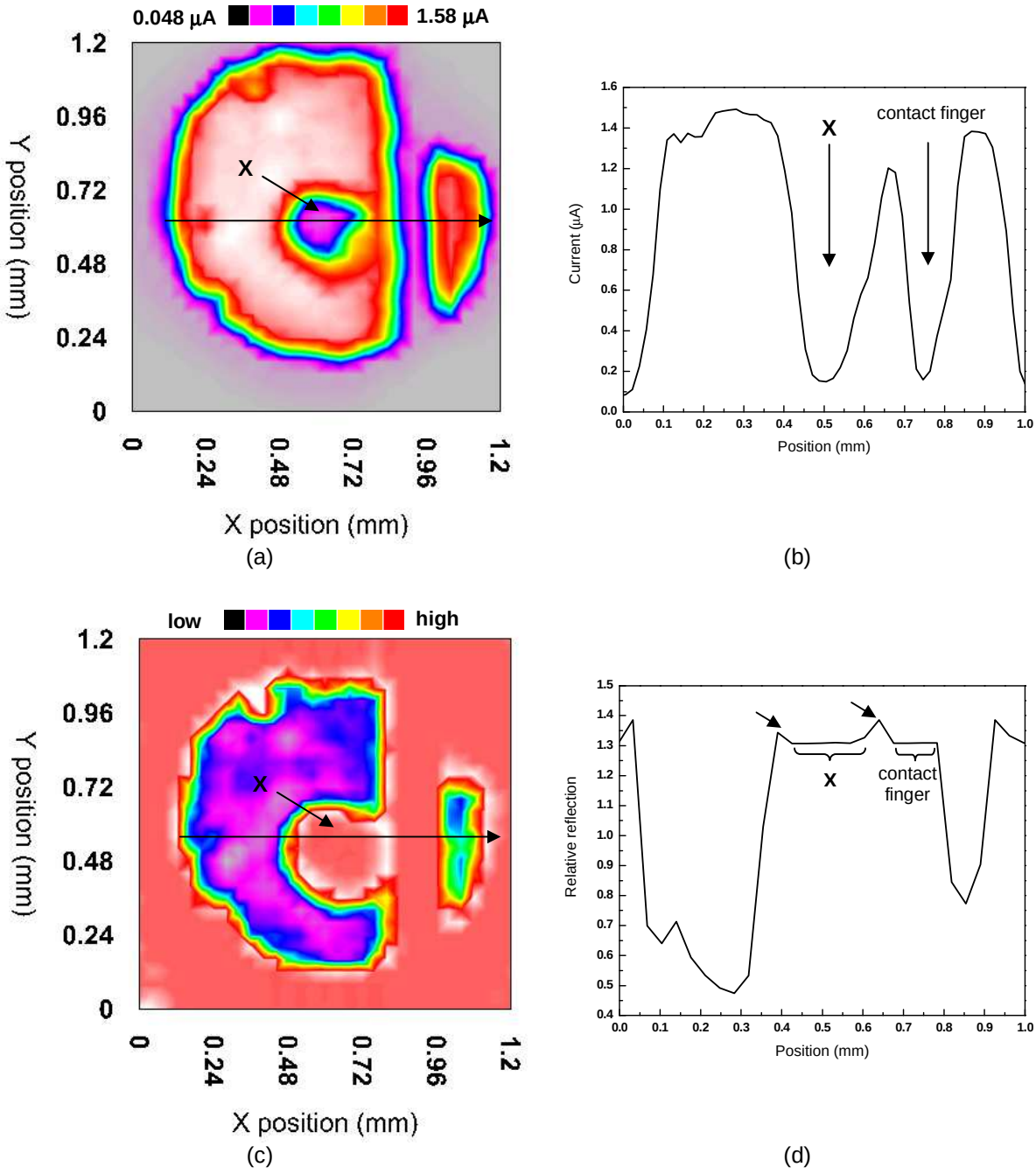

Figure 4: LBIC measurements of the mesa A19 using beam diameter of 100 µm and step size of 50 µm. (a) LBIC map, (b) LBIC line scan, (c) Reflection map, (d) Reflection line scan.

The effect of a surface reflection feature and a grain boundary (GB) that are visible in mesas A19 and V9, respectively, was investigated using LBIC. Fig. 4(a) shows the LBIC current map obtained for mesa diode A19. Fig. 4(c) is the relative surface reflection map of (a). LBIC line scans were performed across the surface as indicated by the arrows in Fig. 4(a) and (c). These line scans are shown in Fig's. 4(b) and (d), respectively. Fig.

5(a) shows LBIC current map of mesa V9. The corresponding line scan taken in the direction indicated by the arrow in (a), is shown in Fig. 5(b). In Fig. 4, a surface defect, indicated by an X, is observed. The effect of region X is characterized by a reduction of photogenerated current at X as shown in Fig 4(a). The magnitude of the current reduction at X is illustrated in Fig. 4(b) and is indicative of the effect of this defect. It can also be seen that the magnitude of the current drop at X is comparable to that of the contact finger. Defect X and similar defects such as those marked by arrows in Fig. 2 shade the cell below resulting in less light reaching the cell, leading to a reduced photo induced current. A solar cell with a significant number of surface defects such as these will produce less current than the others in a module with series-connected solar cells. Such a cell will be reversed biased with respect to other cells and the power produced by other cells with less surface defects will be dissipated by this cell (Wenham, Green & Watt 1995, pp. 73). Dissipation of power in the mismatched cell can increase cell temperature and then give rise to the formation of hot spots, yielding the reduction of cell efficiency (van Dyk et al. 2007). As mentioned above, less light reaches the cell below X indicating that more light is reflected at this defect. To investigate this, the surface reflection measurements shown in Figs 4(c) and (d) are analyzed. In Fig. 4(c) the low reflection is evident in almost the entire areas of the mesa except at the defect X and contact finger which reflect more incident light. The high reflection at X and contact finger is confirmed in the line scan shown in (d). The areas marked by arrows in (c) and (d) show that more light is reflected at the edge of defect X. This suggests that defect X may be caused by a scratch deep into the cell, creating conducting paths that may increase the presence of parasitic resistance. The high R_s and low R_{sh} negatively affect solar cell fill factor (van Dyk & Meyer 2004). The presence of surface defects contributes to degradation of photogenerated current.

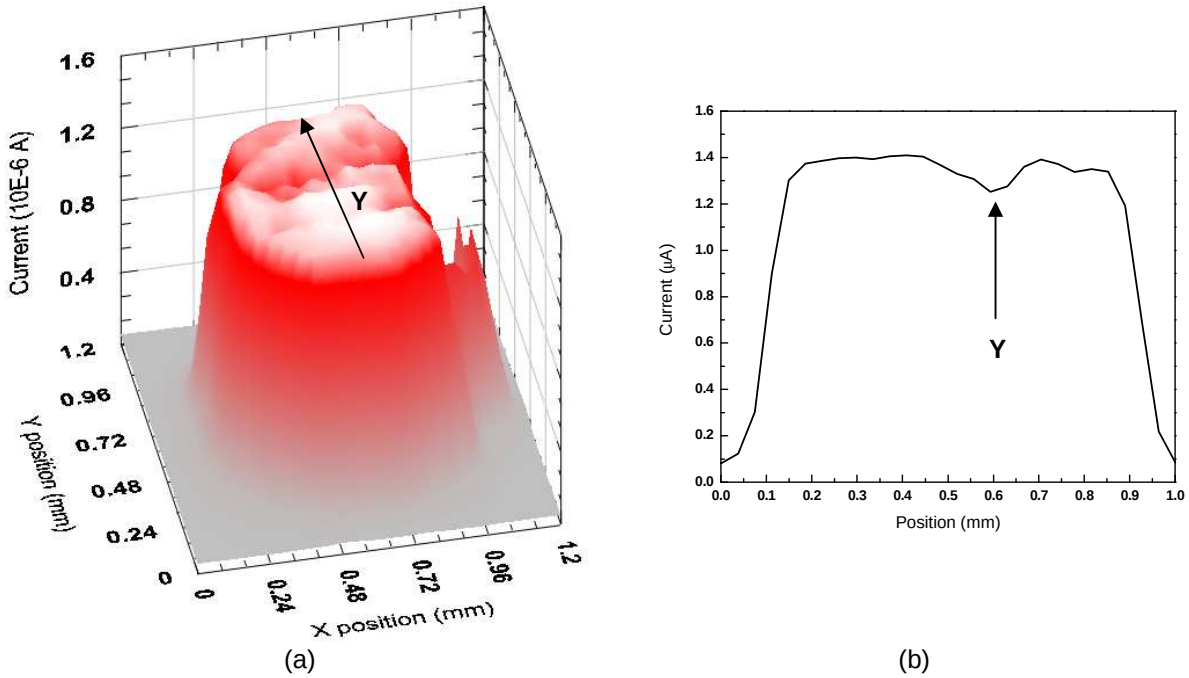

Figure 5: LBIC measurements of the mesa V9 using beam diameter of 100 μm and step size of 50 μm. (a) LBIC map, (b) LBIC line scan.

Another example of a current reducing defect is indicated by region Y as shown in Fig. 5. The current distribution in mesa V9 is depicted in Fig. 5(a) and as expected for multicrystalline material, is not uniform, with the uniformity of current compromised by features such as Y. The effect of feature Y on the current distribution in the entire mesa V9 is analyzed. The low induced current at Y is confirmed by the line scan shown in Fig 5(b). This feature is clearly visible in Fig. 3 and is attributed to a grain boundary. The presence of GBs is typical in multicrystalline based solar cells. Current loss at GBs is due to the formation of space charge layers on the edges of the GB (Das, Arora & Kumar 1985). These layers give rise to electric fields which then control carrier transport. All the minority carriers created within the diffusion length of the GB edge will be attracted and recombine (Das, Arora & Kumar 1985). These recombined carriers will, therefore, not contribute to the collected current.

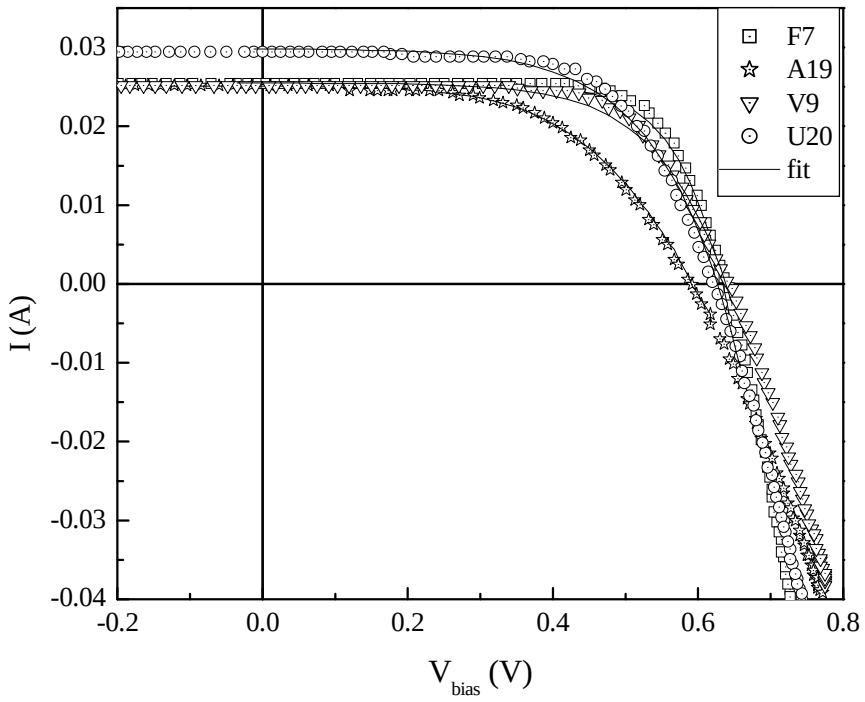

Figure 6: Illuminated I-V curves of the mesa diodes along with the curve fit based on one-diode model.

Further analyses of the mc-Si solar cell mesa diodes were performed by I-V characterization. Illuminated and dark I-V measurements were obtained for the four mesa diodes investigated, viz. F7, A19, V9 and U20. Fig. 6 illustrates the 3-quadrant illuminated I-V characteristics for the mesas and Fig. 7 shows the corresponding dark I-V measurements. Both illuminated and dark I-V measurements allow the determination of device characteristics of the solar cell mesa diodes. In Fig. 6, the slope at I_{sc} and also in the reverse bias region for all of the I-V characteristic remains constant. Similarly, the slope at V_{oc} follows into the negative current region. The V_{oc} of mesa A19 is low

compared to others. The mesa U20 has the highest I_{sc} compared to other three which have similar I_{sc} values. The fitting of the I-V curves was done in the photovoltaic operating region (1st quadrant) using the one-diode model described earlier and the device parameters were extracted. The extracted parameters are summarised in Table 1, with the r^2 values for each fit. The r^2 value gives an indication of the accuracy of the fit.

Table 1: The performance parameters of the mesa diodes.

Mesa	R_s (Ω)	R_{sh} (Ω)	I_o (A)	n	r^2
F7	0.286	621	1.52×10^{-5}	3.11	0.996
A19	0.790	715	2.45×10^{-5}	3.43	0.997
V9	0.295	513	7.80×10^{-6}	3.08	0.993
U20	0.233	286	3.38×10^{-6}	2.79	0.980

Although the fitting for mesa U20 at V_{oc} was not very good, in the regions of interest, i.e. near I_{sc} and V_{oc}, the fits of the other mesas were very good. The I-V characteristic near I_{sc} is influenced by R_{sh} and close to the V_{oc} the I-V curve is affected by R_s (Fonash 1981, pp. 113-114). Therefore, the fit in these regions yields a good estimation of the true values of R_{sh} and R_s. It can be seen that R_{sh} is high for all mesas, but much lower for U20. The lower R_{sh} is indicative of the presence an increase in the shunt paths across the junction of the diode. These shunts give rise to the leakage current which diverts the intended current from the load and hence degrades the performance quality of the cell (McMahon, Basso, & Rummel 1996). It has been reported that within multicrystalline solar cells, transport of current in areas in the vicinity of a grain boundary is influenced by the internal shunt resistance at the grain boundary [8]. From the LBIC measurements, mesa V9 with grain boundary Y, was expected to exhibit high shunting behaviour. However, this was not the case. This could be due to the fact that some grain boundaries act as carrier recombination centres and are weakly charged. It is thus difficult to detect shunt paths in grain boundaries by electrical measurement techniques such as I-V characterization. The extracted R_s values for all the mesas (Table 1) are high. R_s of A19, 0.79 Ω, is higher compared to other mesa diodes and can be attributed to defect X, in agreement with the abovementioned LBIC measurements in Fig. 4. This supports our hypothesis that surface defect X could be damage deep into the top layer of the mesa, contributing to an increase in the effect of parasitic resistances, degrading the performance of the cell [8]. The saturation current, I_0, and ideality factor, *n*, are also listed in Table 1. All the mesa diodes have $n > 2$, and mesas V9 and A19 have the highest ideality factors. The ideality factor reflects the quality of the solar cell junction. As *n* increases the quality of the junction deteriorates. The high *n* of V9 indicates the influence of defect Y in this mesa. The GB (defect Y) could extend through to the p-n

junction, reducing the quality of the junction. In addition, the saturation current, I_0, $2.54\times10^{-5}A$, of mesa A19 is greater than that of the other three mesas. This high I_0 result for the mesa A19 corresponds to the LBIC measurements is expected. In addition to the illuminated I-V characteristics, the dark current density as a function of bias voltage was plotted and is shown in Fig. 7.

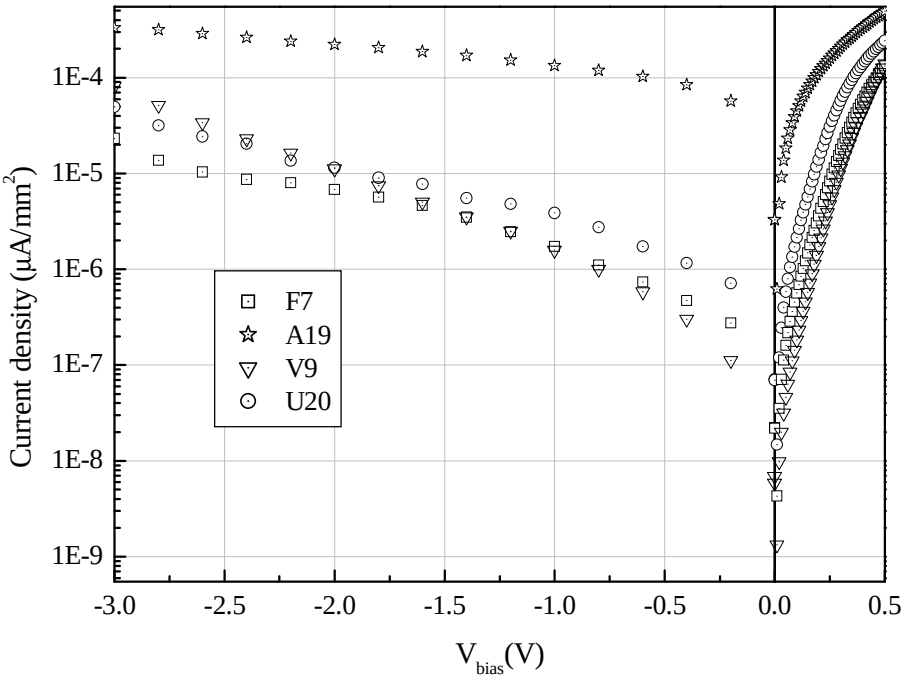

Figure 7: Dark I-V curves of the mesa diodes.

The slope of the forward bias I-V characteristic in the lower voltage range is influenced by R_{sh} while R_s influences the curve at higher voltages (Luque & Hegedus 2003, pp. 102). Only the lower voltage range region of the I-V curve is depicted in Fig. 7. The reverse bias region of the I-V curve gives a good indication of the reverse saturation current I_0 of the cell. In the forward region of the I-V characteristics all the mesas show good rectification except mesa A19, which shows a poor rectifying quality. In the reverse bias of the I-V curves, it can be seen that mesa A19 shows the highest I_0 compared to other mesas. The other three mesas have similar slopes and show relatively similar saturation current. The high I_0 of A19 can be associated with the abovementioned defect X present in this mesa. The high saturation current degrades the open-circuit voltage of the cell (Moller 1993, pp. 35). This agrees with the illuminated I-V characteristic measurements of this mesa. Therefore, surface defects such as X decrease V_{oc} of the cell, resulting in the reduction of the fill factor of the I-V curve. The slope of the dark curve at low voltage suggests that V9 exhibits low shunting. This confirms the results revealed by the illuminated I-V characteristic.

4. Concluding remarks

This paper has shown the value of using mesa diodes to investigate lifetime limiting defects in mc-Si solar cells. The mesas developed on areas of interest within mc-Si solar were analyzed. The results of LBIC measurements and I-V characteristics of mesa diodes were obtained. The LBIC results show that the different defects influence the photogenerated current in a cell. The I-V characteristics of the mesa diodes revealed a quantitative investigation of current transport in the proximity of the isolated defects. The study shows that the mesa diodes can be used to characterize spatial non-uniformities across a crystalline solar cell and directly determine the photovoltaic parameters of the cell as a function of position across the cell.

Acknowledgements

The authors wish to thank the National Laser Centre, Centre for Renewable and Sustainable Energy at University Stellenbosch and Nelson Mandela Metropolitan University Phuhlisa programme for financial support.

References

Das, B.K., Arora, N.K., & Kumar, R. 1985. Effect of impurities & defects on photovoltaic properties of polycrystalline silicon. *Proceedings of the 3rd International Workshop*, Madras, India, pp. 125.

Donolato, C. 1983. Theory of beam induced current characterization of grain boundaries in polycrystalline solar cells. *Journal of Applied Physics*, vol. 54, no. 3, pp. 1314-1322.

Fonash, S.J. 1981. *Solar Cell Device Physics*. Academic Press, New York.

Goetzeberger, A., Knobloch, J., & Voss, B. 1998. *In Crystalline Silicon Solar Cells*. John Wiley, Chichester.

Gosh, A.K., Fishman, C, & Feng, T. 1980. Theory of the electrical and photovoltaic properties of polycrystalline silicon. *Journal of Applied Physics*, vol. 51, no. 1, pp. 446-454.

Luque, A., & Hegedus, S. 2003. *Handbook of Photovoltaic Science and Engineering*. John Wiley and Sons.

Macabebe, E.Q.B., & van Dyk E.E. 2008. Parameter extraction from dark current-voltage characteristics of solar cells. *South African Journal of Science*, vol. 104, pp. 401-404.

Marek, J. 1984. Light-beam-induced current characterization of grain boundaries. *Journal of Applied Physics*, vol. 55, no. 2, pp. 318-326.

Mattiga, A., Capizzi, M., Coluzza, C., & Frova, A. 1988. Oblique grain boundaries: Analysis of light and electron beam induced current profiles in silicon. *Journal of Applied Physics*, vol. 63, no. 9, pp. 4748-4750.

McMahon, T.J., Basso, T.S. & Rummel, S.R. 1996. Cell Shunt Resistance and Photovoltaic Module Performance. *Proceedings of the 25th IEEE Photovoltaics Specialists Conference*, Washington DC, USA, pp. 1291-1294.

Meng, F., Sun, T., & Cui, R. 2000. Recombination properties of grain boundaries in polycrystalline silicon under illumination, *Semiconductor Science & Technology*, vol. 15, pp. 926-930.

Moller, H.J. 1993. *Semiconductors for Solar Cells*. Artech House, Norwood.

Sopori, B.L. 1988. Fabrication of diode arrays for photovoltaic characterization of silicon substrates. *Journal of Applied Physics Letters*, vol. 52, pp. 1717-1720.

van Dyk, E.E., & Meyer, E.L. 2004. Analysis of the effect of parasitic resistances of the performance of photovoltaic modules. *Renewable Energy*, vol. 29, pp. 333-344.

van Dyk, E.E., Audouard, A., Meyer, E.L., & Woolard, C.D. 2007. Investigation of the degradation of a thin-film hydrogenated amorphous silicon photovoltaic module. *Solar Energy Materials and Solar Cells*, vol. 91, pp. 167-173.

Warta, W. 2002. Defect of impurity diagnostics and process monitoring. *Solar Energy Materials and Solar Cells*, vol. 72, pp. 389-401.

Wenham, S.R., Green, M.A., & Watt, M.E. 1995. *Applied Photovoltaic*. University of New South Wales: Centre for Photovoltaic Devices and Systems.